Free Carrier and Many-Body Effects in Absorption Spectra of Modulation-Doped Quantum Wells

GABRIELA LIVESCU, DAVID A. B. MILLER, D. S. CHEMLA, MEMBER, IEEE, M. RAMASWAMY, T. Y. CHANG, MEMBER, IEEE, NICHOLAS SAUER, A. C. GOSSARD, AND J. H. ENGLISH

(Invited Paper)

Abstract—**The large concentrations of free carriers (electrons or holes) present in modulation-doped quantum well (MDQW) samples have important effects on their optical properties. We discuss here the temperature-dependent optical absorption and luminescence spectra of GaAs/AlGaAs and InGaAs/InAlAs n-doped MDQW's with emphasis on the peak seen at the edge of the absorption spectra of these samples. We present here a many-body calculation of the electron–hole correlation enhancement, which identifies this peak with the Mahan exciton—the result of the Coulomb interaction between the photoexcited hole in the valence band and the sea of electrons in the conduction band. This calculation accounts for the strong dependence of the absorption edge peak on both the temperature and the carrier concentration, in good qualitative agreement with our data and with previously published results. We also analyze the changes induced by the carriers on the subband structure through self-consistent calculations, and we conclude that in these symmetric structures, the changes are small for achievable carrier densities.**

I. INTRODUCTION

MODULATION doped quantum wells (MDQW's) are quantum well (QW) structures with the barrier layers doped [1]. The material systems most studied include GaAs wells with AlGaAs barriers, as well as InGaAs wells with InP or InAlAs barriers, lattice matched to InP. The presence of a highly mobile, quasi-two-dimensional (2D) electron or hole gas makes their transport properties extremely attractive for fundamental reasons, as well as from the device point of view [1]. Their optical properties have only recently started to receive more attention [2]–[20], including experiments in photoluminescence (PL) [2]–[7], [20] and photoluminescence excitation (PLE) [2]–[7], magnetoluminescence (ML) [8]–[10], [14]–[16], as well as direct absorption [11]–[13], [17], [18], or absorption saturation under very high photoexcitation [19]. Most of these measurements were done using GaAs/AlGaAs MDQW samples [2]–[13], [19]; data on the InGaAs/InP [14]–[16] and InGaAs/InAlAs [11], [17], [18], [20] material system have become available too, due to the high quality recently achieved for some MDQW samples.

The optical properties of undoped QW's are relatively well understood [3], [21]. At low temperatures, the photoluminescence spectra are often dominated by excitonic recombination between the photoexcited $n_z = 1$ electron and the corresponding heavy hole. The optical absorption spectra of undoped QW's also show well-resolved excitonic resonances at the onset of each intersubband transition. Due to the quantum confinement, there is a large overlap between the electron and the hole wavefunctions, resulting in strong emission and absorption peaks even at room temperature and/or under large applied electrical field, thus making quantum wells highly suitable for electrooptical devices [22].

The mechanisms for luminescence and absorption in modulation-doped quantum wells are much less understood. At low temperatures, the free carriers present in the quantum wells fill the lowest confined states up to the Fermi level E_F (see Fig. 1). For a 2D gas of particles of mass m, $E_F = (\pi\hbar^2/m)N$ where N is the number of particles per unit area (sheet concentration). Since the heavy-hole mass m_{hh} can be 5–8 times larger than the elecron mass m_e (depending on the material), E_F of an electron gas will be 5–8 times larger than that of a hole gas of the same density. This makes effects larger and easier to measure in an n-MDQW, which explains why the vast majority of results reported were obtained on n-doped samples. In the following, we will only be concerned with n-MDQW's, and we will refer to E_F as the electron Fermi energy. For $N = 1 \times 10^{12}$ cm^{-2}, E_F is about 35 meV in GaAs and about 50 meV in InGaAs. This means that the lowest allowed electronic states are occupied up to relatively large in plane wavevectors $k \approx k_F$ on the order of a few times 10^6 cm^{-1}. As a consequence, the electrons that fill these states will participate in the photoemission process, rather than the photoexcited ones (because there are so many electrons already in the sample, the behavior of the photoexcited ones is relatively unimportant). The photoexcited holes, on the other hand, rapidly relax to the top of the valence band, so that the k-conserving vertical transitions that produce the photoluminescence take place essentially at $k \approx 0$, and involve mostly electrons at the bottom of the conduction band (Fig. 1), just as in undoped QW's.

Manuscript received December 22, 1987; revised March 14, 1988.

G. Livescu was with AT&T Bell Laboratories, Holmdel, NJ 07733. She is now with AT&T Bell Laboratories, Murray Hill, NJ 07974.

D. A. B. Miller, D. S. Chemla, T. Y. Chang, and N. Sauer are with AT&T Bell Laboratories, Holmdel, NJ 07733.

M. Ramaswamy was at AT&T Bell Laboratories, Holmdel, NJ 07733. She is with the Department of Electrical Engineering, Massachusetts Institute of Technology, Cambridge, MA 02139.

A. C. Gossard and J. H. English were with AT&T Bell Laboratories, Murray Hill, NJ 07974. They are now with the Department of Materials and the Department of Electrical and Computer Engineering, University of California, Santa Barbara, CA 93106.

IEEE Log Number 8822283.

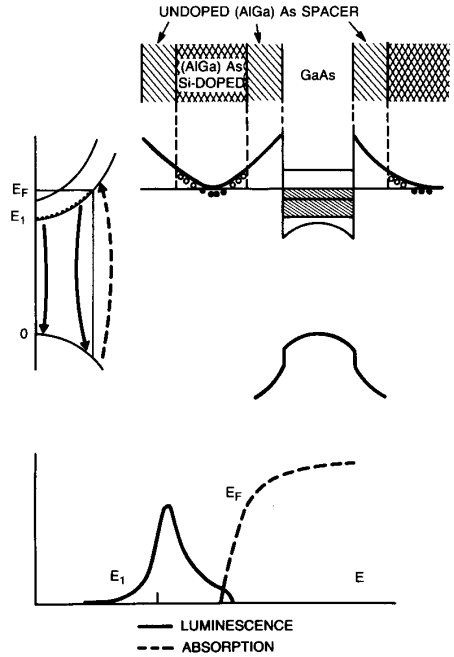

Fig. 1. Schematic description of the absorption and luminescence processes in n-modulation-doped quantum wells. The electrons in the conduction band fill all the states below the Fermi level (dashed area including the first two confined levels). Absorption of a photon (broken arrow) promovates an electron from the valence band to an empty state in the conduction band. Since this state has to be above E_F, the vertical transition involves states with $k \approx k_F$. Luminescence (full arrows) is produced when an electron from the conduction band recombines with a hole in the valence band. Vertical transitions at $k \approx 0$ dominate the observed luminescence spectrum because of the fast relaxation of the photoexcited hole to the top of the valence band, as well as because of the large density of states here. Therefore, the luminescence peak (full line) appears at a lower energy than the onset of the absorption spectrum (broken line).

More information on the nature of the states participating in the recombination process can be obtained by applying a magnetic field H along the z direction. This splits the constant 2D density of states into discrete Landau levels: $E = (l + 1/2)eH/mc$ where m is the mass of the corresponding particle and l is a positive integer. At small magnetic fields, there will be a large number of Landau levels available for electrons below E_F, and recombination will occur between these levels and the corresponding Landau levels of the holes, as shown in ML experiments on GaAs/AlGaAs n-MDQW's [8]–[10]. In InGaAs/InP samples [14], [15], evidence for hole *localization* has been obtained by comparing the transition energies as a function of the applied magnetic field, observed both in luminescence (from electron Landau levels below E_F to the lowest localized hole level) and photocurrent measurements (equivalent to absorption, where transitions occur from hole Landau levels to empty electron Landau levels above E_F). The hole localization (due probably to alloy fluctuations) relaxes the k conservation rules, permitting *all* electrons up to E_F to recombine even at $H = 0$. The luminescence is very broad in this case, covering the energy range between E_1 (the $n_z = 1$ transition) and $E_1 + E_F$ [14].

In absorption spectra, only states *above* E_F will be observed since absorption of light can only be associated with transitions into *empty* electronic states. One thus expects the absorption edge to be shifted to higher energies than in undoped QW's of the same width because it will correspond to vertical transitions at $k \approx k_F$ rather than at $k = 0$. As a consequence, there will be an energy difference between the luminescence and the absorption given by $E_{MB} = (1 + m_e/m_h) E_F$ (similar to the Moss–Burstein shift [23] in doped bulk semiconductors). Low-temperature PL and PLE measurements on n-MDQW's of GaAs/AlGaAs [2]–[7], [11] show that this shift does occur. By electrically tuning the electron concentration in one-sided InGaAs/InAlAs [17], [18], InGaAs/InP [15], [16], or GaAs/AlGaAs [6], [7], the position of the absorption edge can be controlled [17], [18] and this shift can be tuned [6], [7].

There are a number of other features characterizing the luminescence and absorption of MDQW's that cannot be accounted for by the above simplifying "single particle" picture.

1) Although the *shift* of the absorption edge relative to the bandgap E_g can be predicted as a function of N, its *absolute* position cannot because E_g is reduced in the presence of the carriers. This so-called bandgap renormalization is due to many-body effects such as direct and exchange screening [24].

2) Many-body effects must be invoked to explain the line shape of PL spectra. For example, the polarization dependence of the low-temperature luminescence in GaAs/AlGaAs samples [25], [26] can be explained by assuming a significant mixing of the heavy-hole (hh) and light-hole (lh) subbands, even at $k \approx 0$, induced by a "shake up" of the Fermi sea. Similarly, the circular polarization reversal of the low-temperature PL in GaAs/AlGaAs samples when resonantly excited with light at the $n = 2hh$ exciton transition may be explained by the instantaneous buildup of a collective moment of the Fermi sea [4]. Finally, the broad PL to localized holes observed in InGaAs/InP samples [14] had an asymmetric shape, with a strong peak at $E_1 + E_F$. This peak was identified [14] as the many-body Fermi enhancement, analogous to that proposed for degenerate bulk semiconductors and metals by Mahan [27], extensively discussed in the series of papers by Nozieres, Roulet, Gavoret, and deDominicis [28], and observed previously only in the soft X-ray emission and absorption spectra of metals. The luminescence line shape and its temperature dependence could be accounted for by calculations based on the many-body model developed by Schmitt-Rink *et al.* [29], which is applicable, with some minor modifications, to the quasi-two-dimensional case of MDQW's.

3) The single-particle picture alone cannot explain the absorption spectra of MDQW's either. The blue shifted absorption edge is not the $(1 - f_e)$ rectangular step at low temperatures that broadens according to the Fermi–Dirac

distribution f_e at higher temperatures. Instead, a peak is observed at the absorption edge in all low-temperature PLE [2]–[7] or absorption spectra [11]–[13], very similar to the $n_z = 1$ exciton in undoped QW's. At low carrier concentrations [3]–[5], [7], [13], this peak is strong and it still exhibits the characteristic *hh–lh* splitting. As doping increases, the splitting disappears and the peak broadens [2], [6], [7], [11]–[13]. As we will discuss later, when the temperature is raised, the peak rapidly decreases in height and practically disappears for $T > 50$ K, in sharp contrast to the negligible changes of the $n_z = 1$ excitonic line in undoped QW's in this temperature range [30], [31]. This peak was identified as the Fermi edge enhancement due to the many-body electron–hole correlation (the Mahan exciton) [11], [12], [27], [29]. Contrary to the Fermi edge singularity in PL spectra that can only be observed in certain samples where hole localization relaxes k conservation rules, the singularity at the absorption edge is a general, inherent property of MDQW's [11]. We shall discuss this at length below in this paper.

The high-energy structure of the absorption spectra deserves separate discussion. As PLE [3]–[5], [7] and direct absorption [11], [13] measurements have shown, excitonic resonances at the onset of the $n_z = 2$ and $n_z = 3$ transitions can be seen in the spectra of MDQW's also, and over a large range of temperatures, in spite of the screening of the electron–hole Coulomb interaction that might be expected from the free carriers. The explanation of this apparent absence of screening is that the screening is most effective at energies close to E_F where it gives rise to the above-mentioned Fermi edge enhancement [27], [29]. The absence of strong screening for higher transitions is also consistent with time-resolved photoexcitation experiments in undoped samples where strong effects are seen on the $n_z = 1$ exciton with only minor changes at the $n_z = 2$ peak [32]. However, the free carriers do affect the *energies* of all the confined levels via the electrostatic potential present in the sample. The fixed (positive) charge of the ionized dopants (donors) in the barrier layers controls the spatial distribution (the wave function) of the mobile (negative) carriers within the quantum wells. This results in a bending of the bands (see Fig. 1) whose magnitude is given by Poisson's equation and depends linearily on the carrier concentration [1]. In general, $N \leq 1 \times 10^{12}$ cm^{-2} which, if uniformly distributed over a 100 Å wide quantum well with dielectric constant ϵ on the order of 12 (GaAs, InGaAs), produces a maximum bending on the order of 18 meV at the center of the well. This is much less than the barrier heights on the order of 214 meV in GaAs/AlGaAs, 240 meV in InGaAs/InP, and 440 meV in InGaAs/InAlAs. We will evaluate the consequences of this bending specifically below, although the effect of this electrostatic potential is not very large in symmetric structures. It becomes more important, however, in asymmetric, one-sided MDQW's (e.g., FET structures) where it results in an asymmetric distribution of the carriers in the well. The asymmetric skewing of the wells results in substantial shifts of the transitions through the quantum-confined Stark effect [33]. In this case, the screening of the electrostatic field by the mobile carriers is important, and its effect on the confined energies and wavefunctions can be obtained by self-consistently solving the Poisson and Schrödinger equations [5]–[7], [18], [34].

In view of the large amount of data on optical spectra of MDQW's, many of them not yet understood, the time seems appropriate to present them in a unified and comprehensive picture. Our goal in the present paper is to accomplish only part of this ambitious task, namely, to discuss the effect of the carriers on the temperature-dependent absorption and luminescence spectra. We will first present our experimental data (Section II), starting, for the sake of clarity, with results we have obtained in an undoped InGaAs/InAlAs QW sample (Section II-A), which we use as a "control" to compare to doped results. The behavior of the same material system, but modulation doped, is presented in Section II-B, while results on a GaAs/AlGaAs n-MDQW sample are described in Section II-C. The electrostatic effects on the transition energies are described in Section III-A. As mentioned earlier, the existence and the strong temperature dependence of the absorption edge peak in these samples (the Mahan exciton) can be described by means of the 2D many-body model of Schmitt-Rink *et al.* [29]. In Section III-B, we describe briefly our version of the model, slightly modified to describe a single-component plasma of electrons, and we discuss at length the physics behind the model. Finally, in Section IV, we present our conclusions.

II. Experimental Results

A. Temperature-Dependent Absorption and Photoluminescence of InGaAs/InAlAs Undoped QW's

In this section, we present results obtained on a "control" sample—an undoped InGaAs/InAlAs QW structure that is essentially otherwise identical to the doped one. The results we obtain are similar to published data [31], [35], [36] and are essential for the understanding of the results obtained in the modulation-doped sample.

The sample used consisted of 50 periods of 100 Å wide InGaAs wells and 200 Å wide InAlAs barriers, all grown by MBE lattice matched on an InP substrate. The sample was antireflection coated and transmission through it was measured. Examples of our temperature-dependent absorption spectra on undoped InGaAs/InAlAs are shown in Fig. 2(a). The spectra exhibit the typical step-like structure characteristic of the 2D density of states in the confined levels. Excitonic peaks at the edges of each step are clearly seen at all temperatures. The three stronger peaks at 0.855, 1.021, and 1.249 eV seen in the low-temperature spectrum (12 K) are easily identified as transitions between the $n_z = 1, 2, 3$ electron and heavy-hole states E_{1hh}, E_{2hh}, E_{3hh}. The weaker peaks at 0.881 and 1.127 eV correspond to transitions between the $n_z = 1, 2$ electron and light hole states E_{1lh}, E_{2lh}. We calculated the energies corresponding to the above transitions by solving the Schrödinger equation in a finite square well, using the

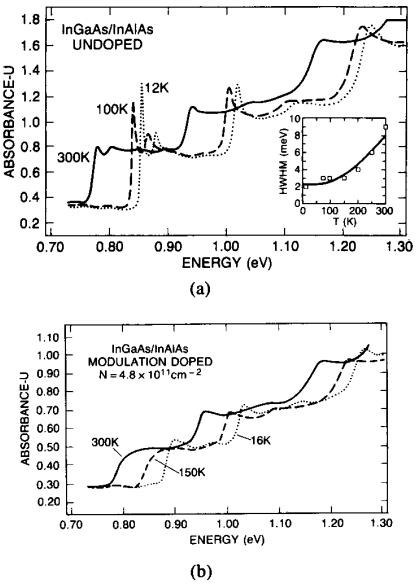

Fig. 2. (a) Temperature-dependent absorption spectra of undoped InGaAs/InAlAs quantum wells. Insert: Half width at half maximum of first absorption peak as a function of temperature. Squares: measured. Curve: calculated (see text). (b) Temperature-dependent absorption spectra of n-modulation-doped InGaAs/InAlAs quantum wells.

TABLE I
PARAMETERS USED FOR THE CALCULATION OF THE ENERGIES OF THE CONFINED STATES (m_0 IS THE FREE-ELECTRON MASS)

	InGaAs/InAlAs	GaAs/AlGaAs
E_g(well)	0.810 eV	1.515 eV
E_g(barrier)	1.543 eV	1.890 eV
ΔE_c	440 meV	214 meV
ΔE_v	293 meV	161 meV
m_e(well)	$0.041m_o$	$0.067m_o$
m_{hh}(well)	$0.377m_o$	$0.340m_o$
m_{lh}(well)	$0.052m_o$	$0.094m_o$
m_e(barrier)	$0.071m_o$	$0.084m_o$
m_{hh}(barrier)	$0.580m_o$	$0.420m_o$
m_{lh}(barrier)	$0.140m_o$	$0.043m_o$

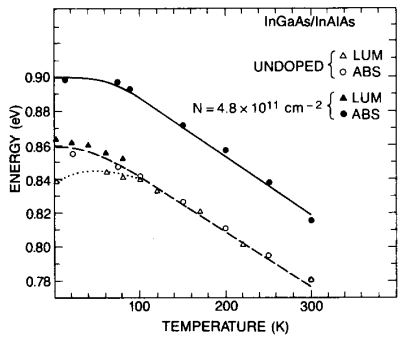

Fig. 3. Position of the luminescence peak (triangles) and first absorption peak (circles) as a function of temperature in the undoped (empty symbols) and doped (full symbols) sample. The lines are guides to the eye.

barrier heights and the electron and hole effective masses as adjustable parameters. The values used for the fit are listed in Table I. They are identical to those reported in [18] and similar to previously reported values [31], [36].

With increasing temperature, the entire absorption spectrum shifts to lower energies, due to the decrease of the bandgap E_g. In Fig. 3, the energies of the E_{1hh} transition are plotted as a function of temperature (empty circles). Above 100 K, a practically linear dependence is observed, with a negative slope of 3.8×10^{-4} eV/K, very close to estimates based on values reported for $\Delta E_g/\Delta T$ in the bulk materials. The excitonic peaks broaden with increasing temperature due to interaction with thermal LO phonons [30], [31]. In the insert of Fig. 2(a), we plotted as a function of temperature the half width at half maximum (HWHM) of the E_{1hh} absorption line (measured on the low-energy side of the peak). The solid line represents a fit to the expression

$$\text{HWHM} = \Gamma = \Gamma_0 + \Gamma_{ph} \Big/ \left(\exp \frac{\hbar\omega_{LO}}{kT} - 1 \right) \quad (1)$$

where Γ_0 is a constant inhomogeneous term accounting for interface roughness and alloy fluctuations, and the second term represents the homogeneous broadening due to scattering by InGaAs phonons. Similar behavior was observed previously in GaAs/AlGaAs samples [30], as well as in earlier measurements on InGaAs/InAlAs samples [31]. Given $\hbar\omega_{\text{LO}} = 35$ meV [31], the best fit we obtain is for $\Gamma_0 = 2.3$ meV and $\Gamma_{\text{ph}} = 15.3$ meV. The inhomogeneous broadening Γ_0 is rather small, indicating a very good sample quality. The value we obtain for Γ_{ph} is significantly larger than that reported in [31] (9 meV), which implies a larger net increase of the linewidth from low temperatures up to room temperature. Since the room temperature width we obtain is roughly the same as the one observed in [31], while the low-temperature width is much smaller in our measurements, we interpret this discrepancy as being partly due to the better quality of our sample and possibly lower errors in measuring Γ.

We also measured the temperature-dependent photoluminescence of the same sample, using the 6471 Å line of a Kr laser for photoexcitation. The energies corresponding to the luminescence peak are plotted as a function of temperature in Fig. 3 (empty triangles). Above $T \approx 100$ K, they coincide with the E_{1hh} energies obtained from the absorption spectra (empty circles in Fig. 3), indicating that the luminescence is excitonic. At low temperatures, however, the luminescence line is Stokes-shifted with respect to the absorption. At $T = 2$ K, the shift is ≈ 15 meV and it decreases with increasing temperature. This dependence is practically identical to that reported for InGaAs/InP QW's [35], and so is the low-temperature line shape of the luminescence. We, too, find that at $T = 2$ K, the luminescence peak is asymmetric to lower energies, with a full width of about 11 meV. This line shape is probably due to low-energy tails of the band densities of states whose participation in the emission pro-

cess is enhanced at low T. Indeed, as the temperature is increased to ≈ 80 K, the luminescence line becomes narrower (7 meV) and acquires the usual asymmetry to higher energies due to the Boltzmann factor. The shift of the luminescence peak to higher energies for temperatures between 2 and 80 K is expected when the luminescence is extrinsic or is due to excitons weakly localized in potential fluctuations [35]; these fluctuations may be caused by variations of the well width or by spatial variations of the alloy concentration. Luminescence from the recombination of localized excitons is predominant at low temperatures. As temperature increases, the excitons become delocalized, and the luminescence arises from band-to-band recombination processes at energies that coincide with the absorption edge peak, as illustrated in Fig. 3.

B. Temperature-Dependent Absorption and Photoluminescence Spectra of InGaAs/InAlAs Modulation-Doped Quantum Wells

The modulation-doped sample has nominally the same structure as the control sample described in the previous section, except that the central 100 Å of the barrier layers is Si doped, leaving 50 Å undoped spacer layers on each side. A carrier density $N = 4.8 \times 10^{11}$ cm^{-2} was obtained from Hall measurements at $T = 2$ K. Absorption spectra obtained at several temperatures are shown in Fig. 2(b). The comparison to Fig. 2(a) reveals striking differences. Although the $n_z = 2$ and $n_z = 3$ transitions can be clearly identified in the spectra of the doped sample too, the strong E_{1hh} and E_{1lh} peaks have disappeared even from the low T spectra, being replaced by a single broad feature, blue shifted by a significant amount (about 40 meV). This blue shift of the absorption edge in the MDQW sample with respect to that of the undoped one is maintained over the whole temperature range, as illustrated in Fig. 3 (full circles, as compared to empty ones). As temperature is increased, the absorption edge peak broadens and disappears rapidly: at 150 K, only a "knee" is left, which barely changes up to room temperature. This broad knee is very similar to the shape described in Fig. 1 for the absorption into the continuum of states above E_F. The higher energy peaks ($n_z = 2, 3$) are observed at energies very similar to the corresponding peaks in the undoped sample (blue shifted by about 5 meV), and they exhibit a larger width even at low temperature. However, the broadening of these peaks from 16 to 300 K takes place at a much slower pace than that of the absorption edge peak. It is quite clear from these spectra already that the absorption edge peak is different in nature from the excitonic peaks seen in the undoped sample.

More information about the origin of the absorption peak may be obtained by comparison to the luminescence data. The luminescence spectrum at $T = 2$ K is presented in Fig. 4. The peak is asymmetric to lower energies, very similar to the line shape observed in the undoped sample. The width of the low energy tail is larger here: about 18 meV (out of a total width of 24 meV) compared to about

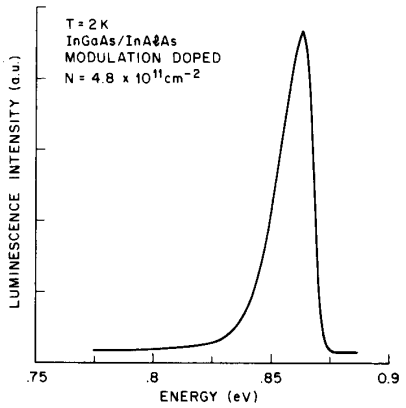

Fig. 4. Low-temperature lunescence spectrum in the modulation-doped InGaAs/InAlAs sample.

6 meV (out of a total width of 11 meV) in the undoped sample, which suggests that bandtails are more populated in the modulation-doped sample. The position of the luminescence peak is also different from that observed in the undoped sample. As illustrated in Fig. 3 (full triangles), the luminescence from the modulation-doped sample is Stokes shifted from the absorption edge by ≈ 38 meV. This value is consistent with the expected Moss–Burstein shift for $N = 4.8 \times 10^{11}$ cm^{-2} and a value for the ratio of the electron and heavy hole in plane masses $m_e/m_h \approx 0.6$ [37].

Two more important pieces of information emerge from Fig. 3. First, the energy of the luminescence peak in the doped sample follows the temperature dependence of the gap, and does not exhibit the initial increase with temperature observed in the undoped sample. This may be a consequence of the large concentration of electrons at the bottom of the conduction band in the doped sample that exceeds by far the small concentration of weakly localized carriers that were participating in the recombination process in the undoped sample. One may conclude, therefore, that even at low T, the luminescence we observe in the modulation-doped sample is intrinsic, due to band-to-band recombination. Second, the luminescence peak not only follows the temperature dependence of the absorption edge in the undoped sample, but it also occurs at practically the same energy. There is a small, but systematic, blue shift of about 5 meV which, together with the 5 meV blue shift of the $n_z = 2$ and $n_z = 3$ transitions, suggests that all the transitions in the modulation-doped sample occur at the same energies as in the undoped one. This is consistent with the fact that the two samples have essentially identical structure. The small difference in energies may be due to strain or slight differences in the widths of the quantum wells in the two samples. It also suggests that: 1) the bandgap renormalization effects are small at this concentration, and 2) the bending of the bands due to the charges present in the MDQW sample (see Fig. 1) has a negligible effect on the transition energies. We will discuss the latter in Section III-A.

C. Temperature-Dependent Absorption and Photoluminescence of GaAs/AlGaAs Modulation-Doped Quantum Wells

We have done the same type of measurements using a GaAs/AlGaAs n-MDQW sample [11]. The structure consisted of 120 Å quantum wells, sandwiched between 350 Å barriers, whose central 115 Å is Si doped (n type). A concentration $N = 2.6 \times 10^{11}$ cm^{-2} was obtained from low-temperature Hall measurements. Examples of the absorption and luminescence spectra are shown in Fig. 5(a). Similarly to the previous material system, the low-temperature absorption spectrum (10 K) shows the $n_z = 2$ and $n_z = 3$ transitions, while the strong E_{1hh}, E_{1lh} peaks characteristic for the spectra of undoped samples are replaced here by a single peak. A blue shift of this peak with respect to the luminescence is also observed. The value of the shift is $E_{MB} \approx 15$ meV, which corresponds to $N = 3.5 \times 10^{11}$ cm^{-2}, using $m_e/m_h = 0.2$ for the electron to heavy hole in plane mass ratio [2]. The value we obtain for N is somewhat higher than that measured by Hall effect, which could be due to inhomogeneities of the doping over the area of the wafer. A fit of the transition energies was performed, solving the Schrödinger equation in a square well with the parameters listed in Table I. The reason for using a square well, neglecting the electrostatic "bending" of the bands, is explained in Section III-A. The calculated transition energies are indicated with arrows in Fig. 5(a). Bandgap renormalization of 12 meV was assumed in this calculation for all transitions. As in the case of InGaAs/InAlAs sample, the luminescence corresponds to the E_{1hh} transition.

With increasing temperature, the absorption peak decreases and broadens, as in the previous sample. But the changes are more spectacular here since the peak is much sharper to begin with. As can be seen in Fig. 5(b), an increase in temperature of 50 K is enough to nearly double its linewidth. This should be compared to the situation in the undoped GaAs/AlGaAs quantum wells where a temperature of 300 K was necessary to broaden the E_{1hh} absorption line by the same amount.

With increasing temperature, the entire spectrum shifts to lower energy, like in the previous samples. In Fig. 5(c), the positions of the luminescence and the first absorption peak are plotted as a function of temperature. Note that for temperatures above 100 K, the energy difference between them decreases, becoming practically zero at room temperature. This may be rationalized as being due to the temperature dependence of the Fermi energy or, more precisely, the chemical potential

$$E_{\text{chem}} = kT \ln\left(\exp\frac{E_F}{kT} - 1\right) \qquad (2)$$

(where E_F is the chemical potential at $T = 0$). In Fig. 6, the calculated values of E_{chem} are plotted as a function of temperature for different concentrations N. The dots represent the experimental values, obtained from the energy difference between the positions of the absorption edge and the luminescence peak. There is a good agreement for $N = 3.5 \times 10^{11}$ cm^{-2}.

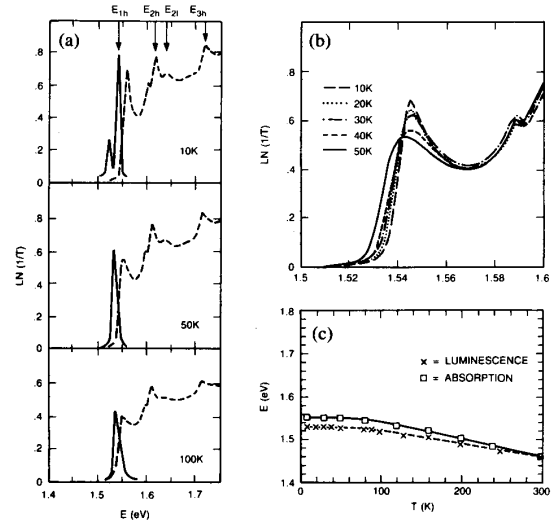

Fig. 5. (a) Absorption (broken line) and photoluminescence spectra (full line) of the GaAs/AlGaAs n-modulation-doped sample. The arrows on the top spectrum indicate calculated transitions. (b) First absorption peak as a function of temperature on an extended scale. (c) Temperature dependence of the positions of the luminescence peak (crosses) and first absorption peak (squares).

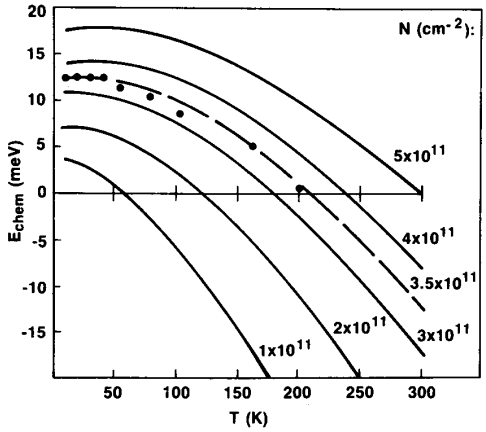

Fig. 6. Full lines: calculated temperature dependence of the chemical potential in an n-modulation-doped GaAs/AlGaAs quantum well for different carrier concentrations N. Dots: experimental points, obtained from the energy difference between the luminescence peak and the first absorption peak in the GaAs/AlGaAs sample [see Fig. 5(c)]. Broken line: the curve that fits the data.

Summarizing this section, we conclude that the main features characterizing the optical spectra of modulation doped quantum wells are as follows.

1) There is a difference in energy between the luminescence and the absorption edge. At low temperature, it can be well approximated by the Moss–Burstein shift $E_{MB} = (1 + m_e/m_h)E_F$, should be replaced with E_{chem}.

2) The absorption edge exhibits a peak, which is strongly temperature dependent. Its behavior is not con-

sistent with that of a conventional exciton in an undoped quantum well structure.

3) The higher energy absorption peaks appear in the spectrum at approximately the same positions as in an undoped sample with the same structure. Their width is larger in the doped samples. Temperature effects on these peaks are by far weaker than in the case of the edge peak.

We shall discuss these results in the following section. In Section III-A, we calculate the confined energy levels in the presence of the charges to find out at what concentrations and to what extent these electrostatic effects become important. In Section III-B, we discuss the nature of the absorption edge peak. We show that it can be identified as the many-body electron–hole correlation singularity whose existence was predicted by Mahan for degenerate, bulk semiconductors [27]. We follow a 2D version of this calculation, developed by Schmitt-Rink *et al.* [29] and we calculate the line shape of this peak, as well as its dependence on temperature and carrier concentration.

III. Discussion

A. Self-Consistent Calculation of the Transition Energies in a Modulation-Doped Quantum Well

In order to check the effect of the electrostatically produced band bending on the confined levels, we have self-consistently solved the Poisson and Schrödinger equations in this type of structure. The calculation is similar to that described in [34]. As a starting point for the iteration, we assumed that the free electrons were initially distributed in the quantum well according to the wave function of the $n_z = 1$ unperturbed state, which was calculated using a tunneling resonance program. This approxmation is valid at low temperatures and for carrier concentrations such that E_F is smaller than the difference between the $n_z = 2$ and the $n_z = 1$ electronic levels. For InGaAs, this condition restricts the calculation to $N < 3 \times 10^{12}$ cm^{-2}, and in GaAs to $N < 2 \times 10^{12}$ cm^{-2}. These maximum values are well above the concentrations in the present samples. We then solved the Poisson equation assuming the ionized donors to be uniformly distributed in the doped regions of the barriers. We superposed the electrostatic potential obtained in this way on the original square well, thus "bending" the bands (see Fig. 7). In the next iterations, we found the confined levels in this new "bent" well, and we redistributed the electrons accordingly (in the newly found $n_z = 1$ state). The procedure converged rapidly: after five iterations, the changes in the energy of the first electronic level were less than 0.5 meV. With the electrons populating the $n_z = 1$ level obtained from the last iteration, we recalculated the electrostatic potential, found the other confined levels (for electrons, heavy holes, and light holes), and calculated the transition energies.

In Fig. 7, illustrative results of the calculation performed using parameters of InGaAs/InAlAs are shown. The structure consisted of a 100 Å well, sandwiched between 200 Å barriers, whose central 100 Å were doped. The structure and the resulting potential for the highest electron concentration used ($N = 2.5 \times 10^{12}$ cm^{-2}) are described in Fig. 7(a). The potential in the undoped structure is plotted using broken lines, while the potential cal-

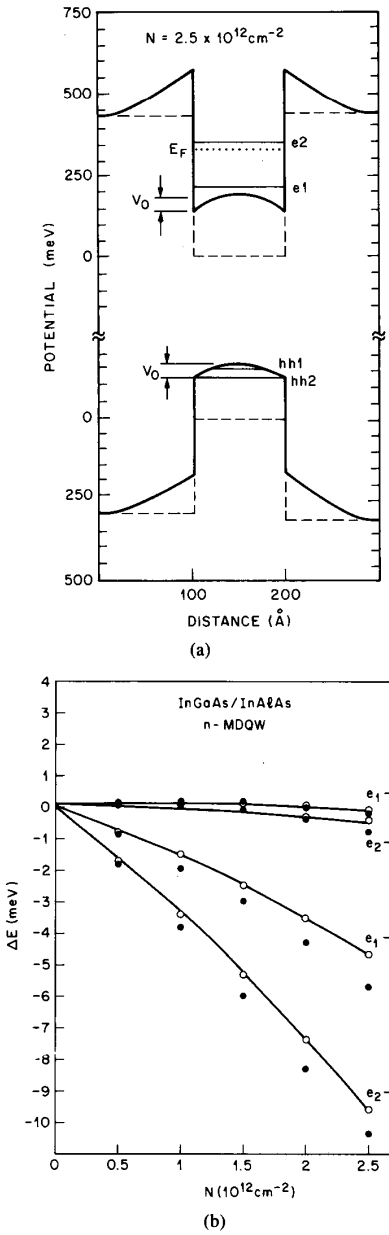

Fig. 7. Electrostatic effects in a modulation-doped quantum well structure. (a) Band structure of the quantum well. Broken line: undoped. Full line: Potential obtained from the self-consistent calculation (see text). V_0 represents the maximum bending at the center of the well. E_F indicates the position of the Fermi level, e_1, e_2, hh_1, hh_2 indicate the positions of the confined levels of the electrons and heavy holes, respectively (in presence of the charge). (b) Calculated shifts ΔE of the transition energies as a function of the carrier concentration N. Empty circles: homogeneously distributed charges. Full circles: self-consistent calculation (see text). The lines are guides to the eye.

culated for the doped structure is plotted with full lines. Only 100 Å of each barrier are shown. The positive charge of the ionized donors is distributed in the first and last 50 Å of the barriers, while the negative charge is distributed according to the wave function of the confined electrons in the well. The energy levels corresponding to the $n_z = 1$, 2 electron and heavy-hole confined states in the presence of the charge are indicated, as well as the Fermi level E_F. The $n_z = 3$ electron level is not shown because, being so close to the top of the well, it becomes unbound for relatively small carrier concentrations. The maximum bending at the center of the well is proportional to the carrier concentration. We calculate the band bending exactly in our self-consistent calculation below, but it can be well approximated by the "uniform charge density" result $V_0 = 1/2\ (\epsilon\rho z^2)$ where ρ is the volume carrier density and z is measured from the edge of the well. For $\epsilon \sim 12$, this gives $V_0 \sim 17$ meV at the center of the well for $N = 1 \times 10^{12}$ cm^{-2} ($\rho = 1 \times 10^{18}$ cm^{-3}) and $\sim$43 meV for $N = 2.5 \times 10^{12}$ cm^{-2} ($\rho = 2.5 \times 10^{18}$ cm^{-3}). These values are not very large when compared to the barrier heights, but are significant when compared to the energies of the lowest confined levels in the undoped quantum well: 48 meV from the bottom of the conduction band for the electron, 7 meV from the "bottom" of the valence band for the heavy hole, and 32 meV for the light hole.

The effect of the band bending is obtained by calculating the transition energies in the presence of the band bending and comparing them to the values obtained for the square undoped quantum well. In Fig. 7(b), we plot the differences ΔE between the transition energies calculated with and without the charges as a function of the carrier concentration N for the transitions involving the $n_z = 1$, 2 electron, heavy hole, and light hole states (full circles). It can be seen that the values ΔE are very small (on the order of a few meV) at the concentrations present in our samples, becoming significant only at concentrations above 10^{12} cm^{-2}. The differences are negative and approximately linear in N for the case of the heavy-hole transitions where clear shifts are predicted. In the case of transitions involving the light holes, there is practically no change ($\Delta E \approx 0$) over the whole range of concentrations.

The reason for these extremely small changes is the fact that the effects of bending up the bottom of the conduction band and bending down the "bottom" (as seen by the holes) of the valence band tend to cancel each other. This can be deduced from first-order perturbation theory, which is applicable here since the changes ΔE are proportional to N, and thus to the perturbation V_0. The correction to the energy of the confined levels from a parabolic bending within the wells can be written as $E_i^{(1)} = \langle \Psi_i^{(1)} | az^2 | \Psi_i^{(0)} \rangle$ where $i = e$, hh, lh, the constant a is proportional to the carrier concentration, and z is the distance. This expression has always the sign of a: it will be negative for $a < 0$ [bending upwards of the bottom of the conduction band; see Fig. 7(a)] and it will be positive for $a > 0$ [bending "downwards" of the "bottom" of the valence bands; see Fig. 7(a)]. Its value will also be linear in a, of course, which in this case means linear in N. The transition energy is calculated as the sum between the energy of the gap E_g and the energies of the electron and hole, measured with respect to the bottoms of their corresponding wells. The change in the transition energy will therefore be $\Delta E = E_e^{(1)} + E_{\text{hole}}^{(1)}$, with $E_e^{(1)}$ negative and $E_{\text{hole}}^{(1)}$ positive. Were the absolute values of $E_i^{(1)}$ equal, they would cancel each other and $\Delta E = 0$. This happens in the case of the light hole [see Fig. 7(b)] because the wavefunctions $\Psi_e^{(0)}$ and $\Psi_{lh}^{(0)}$ are very similar (the particles have similar masses). In the case of the heavy hole, the masses are very different (the ratio $m_{hh}/m_e \approx 10$; see Table I), and so are $\Psi_e^{(0)}$ and $\Psi_{hh}^{(0)}$. Therefore, a larger shift is expected and obtained, as shown in Fig. 7(b). The fact that ΔE is negative shows that the dominant shifts are those of the electronic levels.

The self-consistent calculation has an interesting effect on the $n_z = 1$ electronic wavefunction: Ψ_e "spreads" along z, the direction perpendicular to the quantum well, as a result of the electrostatic attraction of the electrons to the positively charged barriers, which tends to screen the electrostatic field. Actually, almost identical solutions for the Schrödinger equation are obtained if one approximates the electrostatic potential with that created by *uniformly* distributed negative charge in the well too. To illustrate this, we have plotted in Fig. 7(b) also the energy differences ΔE calculated assuming a uniform distribution for the electrons in the QW's (empty circles). The values obtained for ΔE from the two calculations are very close, within 0.5–1 meV from each other for all the concentrations considered. This error is actually of the same order of magnitude as the fluctuations of the energy level during the iteration. The fact that the results of the self-consistent calculation are always below those obtained assuming the charge homogeneously distributed is probably due to the fact that we stopped after a small number of iterations, with a slightly asymmetric wavefunction for the electron. This asymmetry is similar to the application of a small electric field, which slightly skewes the well and shifts all transitions to lower energies.

Our conclusion is therefore that an excellent approximation of the electrostatic potential in a symmetrical modulation-doped structure can be obtained by assuming that the free carriers are homogeneously distributed within the quantum wells. Consequently, there is in practice no need for time-consuming self-consistent calculations to obtain the confined levels and wavefunctions in these symmetrical structures.

From these calcuations, we also arrive at a second conclusion: the shift of the interband transition energies as a function of N is negligible for concentrations below 10^{12} cm^{-2}. Therefore, a calculation of the transition energies in a *square* well is an excellent approximation in a symmetric structure, moderately doped.

B. Many-Body Effects in the Absorption Spectra of Modulation-Doped Quantum Wells: The Fermi Edge Correlation Singularity

We discuss in this section the nature of the absorption edge peak and its dependence on temperature and carrier concentration. We present a many-body calculation of the absorption edge line shape which accounts for the existence of this peak at the Fermi edge, and predicts a dependence on temperature and carrier concentration that agrees with the experiment.

The relatively large concentration of electrons in the conduction band of a modulation-doped quantum well can be regarded as a degenerate electron gas. Their screening of the Coulomb interaction should drastically weaken the interaction between photoexcited electrons and holes, eventually leading to the disappearance of the excitonic resonances from the absorption spectrum. As first demonstrated by Mahan [27], excitonic effects persist in principle even into regions where the conduction band is a high density gas. He showed that, were it not for lifetime broadening, a real electron–hole bound state would exist, which would appear in the optical spectrum at an energy close to the Burstein edge, and whose binding energy would vanish at very large concentrations. The existence of the bound state is related to exclusion principle restrictions on the electrons' scattering. The experimental observation of this Fermi edge resonance in doped bulk semiconductors is practically impossible because of the strong scattering of carriers by the random impurity potentials. One way of creating large densities of charge carriers without the introduction of impurities in pure bulk semiconductors is by optical excitation: at sufficiently large intensities, an electron–hole plasma is created. Using this technique, Asnin *et al.* [38] seem to have observed this Fermi resonance as a weak enhancement at the absorption edge of pure Ge. The crucial aspects of modulation-doped quantum wells that make possible the observation of the Fermi edge resonance are, we believe, the spatial separation between the ionized donors in the barriers and the carriers in the wells, on one hand, and the enhancement of the oscillator strength of the absorption due to confinment of the carriers in the quantum wells, on the other.

A full theoretical treatment of the Fermi edge resonance is very complicated, as discussed at length by Nozieres *et al.* [28] for the case of metals, and by Ruckenstein and Schmitt-Rink [29] for semiconductors. The conclusion they reach for both cases is that the singularity exists, although the calculation of the line shape is outside the scope of conventional perturbation theory. In the approximate treatment of Mahan [27] (used for quantum wells by Schmitt-Rink *et al.* [29]), the absorption process is viewed as the optical creation of an electron–hole pair, and the Coulomb scattering between the photocreated hole and the sea of electrons is calculated in the final state. This scattering causes a logarithmic singularity in the absorption spectrum at E_F, which decreases in intensity as the carrier concentration increases, and is smoothened by the finite lifetimes of the electrons and holes. The only electron–hole scattering terms used in this calculation are the so-called "ladder diagrams" which, for an insulating semiconductor, are identical to Eliott's method of solving the hydrogenic Schrödinger equation [27]. Other types of terms, the "nonladder diagrams," will also affect the optical absorption. As predicted by Mahan [27], there is no possibility that these terms will cancel the logarithmic singularity. Nozieres *et al.* [28] confirmed later that these corrections practically cancel each other, thereby having little effect on the shape of the Fermi edge spectrum in metals. Therefore, in our attempt to calculate the absorption edge line shape, we have used the approximate many-body 2D model developed by Schmitt-Rink *et al.* [29], which essentially applies Mahan's approach to electron–hole plasmas in highly photoexcited quantum well structures. In their model, the optical spectra are obtained by solving the Bethe–Salpeter equation (BSE) for the *e–h* pair Green's function within the statically screened ladder approximation. This singular integral equation describes the multiple scattering of electrons and holes via the statically screened Coulomb interaction. In our modified version, the plasma is composed of electrons only. This affects the screening of the Coulomb interaction, and therefore the electron and hole eigenstates, as well as the interband density of states, which determines the absorption coefficient α. In order to calculate the expression of the absorption coefficient, we therefore went step by step through the calculation of [29], only adapting it for the single component plasma of electrons. In the following, we briefly recall these steps, and we devote more space to the discussion of the physics behind this model.

The carriers interact via the 2D Coulomb interaction $V(r) = e^2/\epsilon_0 r$ where ϵ_0 is the background dielectric constant. In the absence of carriers, the photoexcited electrons e and holes h form excitons, with 2D binding energy $E_{2D} = 2me^4/\hbar\epsilon_0^2$ and Bohr radius $a_{2D} = \hbar\epsilon_0/2me^2$ where m is the reduced electron–hole mass: $m^{-1} = m_e^{-1} + m_h^{-1}$. We consider here the heavy hole only. In the presence of free carriers (electrons, in our case), one has to include exchange effects as well as the screening of the Coulomb forces. The 2D screened Coulomb interaction can be expressed as $V_s(q, \omega) = 2\pi e^2/\epsilon(q, \omega)q$.

Following [29], we use the static random phase approximation (RPA) for the dielectric constant $\epsilon^{-1}(q, o) = \epsilon_0^{-1}(1 - (\omega_p^2(q)/\omega^2(q)))$. Here $\omega_p(q)$ is the 2D plasma frequency $\omega_p^2(q) = 2\pi Ne^2q/\epsilon_0 m_e$ where N is the electron concentration (per unit area). $\omega(q)$ is the frequency of the effective plasmon mode: $\omega^2(q) = \omega_p^2(q)(1 + q/\kappa) + q^4\hbar^2/4\,m_e^2$. The screening wavenumber κ is given by $\kappa a_0 = m_e/m\,[1 - \exp(-(E_F/kT))]$ where $E_F = \hbar^2k_F^2/2m_e$ and $k_F = \sqrt{2\pi N}$. Finally, $\epsilon(q)$ becomes

$$\frac{\epsilon(q)}{\epsilon_0} = 1 + \frac{1}{qa_0}\left[(\kappa a_0)^{-1} + \frac{m}{m_e}\frac{(qa_0)^2}{2k_F^2}\right]. \quad (3)$$

Note that the screened Coulomb interaction $V_s(q)$ depends both on temperature and on carrier concentration via κ, and that contrary to the unscreened case, $V_s(q = 0)$ does not diverge and its value is $2\pi e^2/\epsilon_0\kappa$. At a given T, as the concentration increases, κ and hence ϵ become larger, making the screening more efficient. Changes in temperature also have an important effect on $V_s(q)$: for a given concentration of carriers, increasing T makes κ and ϵ smaller, which in turn makes the screening less effective and $V_s(q = 0)$ becomes larger.

The absorption spectrum associated with optical transitions between the lowest electron and hole subbands is determined [29] by the interband density of states $D(\hbar\omega)$. In the absence of carriers,

$$\alpha(\hbar\omega) = D_0(\hbar\omega) = \pi \sum_n \left|\phi_n(r = 0)\right|^2 \delta(\hbar\omega - E_n) \tag{4}$$

where E_n are the eigenvalues of the unperturbed excitonic problem, corresponding to the wavefunctions $\phi_n(r)$ and $\phi_n(k)$ in real and reciprocal space, respectively. (The sum is carried over both the discrete states and the corresponding continua.) In the presence of free carriers, one has to replace the excitonic eigenfunctions $\phi_n(k)$ by scattering (i.e., unbound) states $\phi_p(k)$, classified according to the relative e–h momentum p. The electron–hole pair energies are $E(p) = E_e(p) + E_h(p)$, depending now on a continuous index p, and not the discrete index n, which characterized previously the excitonic e–h states. The interband density of states (i.e., the absorption coefficient α) is calculated as [29]

$$\alpha(\hbar\omega) = D(\hbar\omega) = D_0(\hbar\omega)\,\rho(\hbar\omega) \tag{5}$$

where $D_0(\hbar\omega) = 1 - f_e(\hbar\omega)$ represents the one particle result, and

$$\rho(\hbar\omega) = \left|1 - \frac{\lambda_2(p)}{\lambda_1(p)}\right|^2_{E(p)=\hbar\omega} \tag{6}$$

is the correlation enhancement due to multiple e–h scattering. Here $\hbar\omega$ is the photon energy, and λ_1 and λ_2 are given in the limit of moderate densities ($Na_{2D}^2 < 1$) and low temperatures ($kT/E_{2D} < 1$) by the following expressions:

$$\lambda_1(p) = \frac{1}{V_s(p, p)} \sum_k \left[V_s(p, k)\right]^2 \frac{1 - f_e(k)}{E(p) - E(k) + i\delta} \tag{7}$$

$$\lambda_2(p) = \sum_k V_s(p, k) \frac{1 - f_e(k)}{E(p) - E(k) + i\delta} \tag{8}$$

where

$$V_s(k, k') = \frac{1}{2\pi} \int_0^{2\pi} d\rho\, V_s(\vec{k} - \vec{k}')$$

is the angle-averaged value of the statistically screened Coulomb interaction (ρ is the angle between $\vec{k}$ and $\vec{k}'$). The use of the angle averaging is justified by the fact that only s-wave scattering states [29] are contributing to $D(\omega)$.

These expressions include terms containing the screened 2D Coulomb interaction, as well as the distribution function of the screening particles. Therefore, both $D_0(\hbar\omega)$ and $\rho(\hbar\omega)$ depend on the temperature T and concentration N. Using (5)–(8), we have calculated the correlation enhancement $\rho(\hbar\omega)$ and the absorption coefficient $\alpha(\hbar\omega)$. In Fig. 8, we have plotted the results of the calculation of for GaAs: values of α in the temperature range 10–50 K (kT/E_{2D} between 0.05–0.27) are plotted in Fig. 8(a) for a fixed value $N = 3.5 \times 10^{11}$ cm^{-2} ($Na_{2D}^2 = 0.15$), while in Fig. 8(b), the absorption coefficient is calculated as a function of the concentration N at a fixed temperature $T = 10$ K. The horizontal axis in the figure is the photon energy, measured from the energy gap between the top of the $n_z = 1$ hole subband and the bottom of the $n_z = 1$ electron subband. Apart from universal constants, the only numerical inputs used are the masses m_e and m_h, the temperature T, and the electron concentration N.

It is clear that we are able to reproduce qualitatively the behavior observed in the experiment: at an energy equal to $(1 + m_e/m_h)E_F$, the spectra exhibit a peak, which weakens rapidly when temperature is increased. This peak reflects the behavior of the correlation enhancement $\rho(\hbar\omega)$. It is a result of the interaction between the hole created in the valence band and the electron gas in the conduction band. The movement of the sea of electrons towards the hole, which screens the Coulomb potential of the hole, of itself correlates them together, thus enhancing the absorption. Hence, the correlation is actually caused by the screening mechanism. The correlation factor is strong and narrow at low temperatures, becoming singular at $T = 0$. (An arbitrary broadening $\delta = 1$ meV was introduced to avoid the singularity in the numerical integration used in calculating λ_1 and λ_2.) The screening (and the correlation) becomes weaker as the hole wavevector moves away from k_F, and hence the spectral peak around the Burstein edge. The screening (and the correlation) also becomes weaker with increasing temperature, and hence the thermal broadening of $\rho(\hbar\omega)$, which reflects the thermal broadening of the electrons' distribution function.

It is interesting to note that this result is most unexpected in the framework of the single particle picture. One would have expected the electron plasma to effectively screen the hydrogenic exciton at low temperature. At higher temperatures, one would have expected to see a reappearance of the excitons, as a result of the weakened screening. The experiment shows that the opposite is true for the present density: at low temperature, a strong peak is seen in the absorption spectra due to the fact that the electron gas forms a correlated state with the hole, a collective analog of the hydrogenic exciton in an undoped sample. At higher temperatures, as the electrons are spreading in energy, the peak weakens because this correlation weakens, analogous to the "unbinding" of a

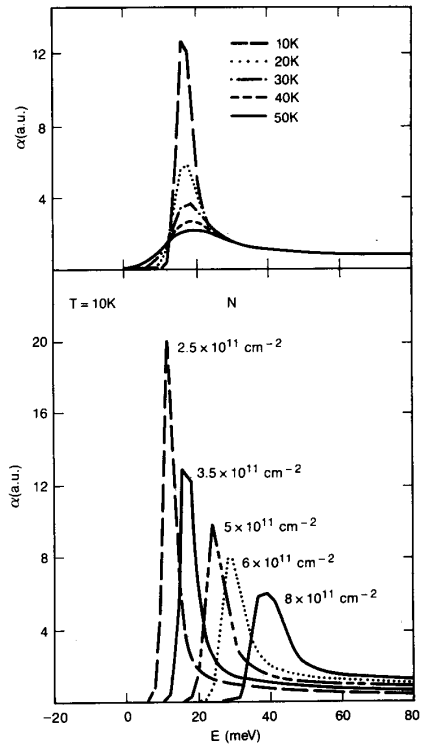

Fig. 8. Calculated absorption coefficient for the GaAs/AlGaAs n-MDQW structure. Upper: absorption edge peak as a function of temperature for $N = 3.5 \times 10^{11}$ cm^{-2}. Lower: absorption edge peak as a function of carrier concentration for $T = 10$ K. Horizontal axis: energy measured from E_{1h}, the energy gap between the top of the $n = 1$ heavy-hole subband and the bottom of the $n = 1$ electron subband.

state. In fact, the hydrogenic exciton and the correlation singularity can be regarded as two extremes of the same Coulomb enhancement phenomenon, the exciton representing the case of maximum screening of the hole by one electron.

The effect of the carrier density on the absorption edge peak is shown in Fig. 8(b). The calculated absorption coefficient at $T = 10$ K is plotted for different values of N up to $N = 8 \times 10^{11}$ cm^{-2} ($Na_{2D}^2 = 0.34$). It can be seen that for increasing carrier densities, the maximum of $\alpha(\hbar\omega)$ near the chemical potential decreases, reflecting the decreasing e–h coupling due to increased phase space occupation and exchange effects [24], [29]. This agrees with the behavior observed in the spectra of n-MDQW's of GaAs/AlGaAs [7], [13]: with increased doping, the E_{1hh} and E_{1lh} absorption peaks broaden and eventually merge into one single, broad peak. The fact that there is only one peak left in the absorption spectra is due to the mixing of the heavy hole and the light hole for wavevectors $k \approx k_F$ [7], [11].

The line shapes we calculate for α are much narrower than the actually observed ones, which limits our agreement to a qualitative one. The reason is that we have not included any broadening mechanisms in our calculations, such as inhomogeneous broadening or the contribution of the light hole, none of which is easily modeled. The fact that this calculation is valid only at low temperatures justifies our neglect of the phonon-induced broadening too. In fact, this whole calculation was essentially performed in order to explain the strong temperature dependence of the absorption coefficient in a range where the optical phonon interaction is practically nonexistent. Finally, we wish to emphasize one source of broadening that is *not* present experimentally: broadening from collisions with ionized impurities. This is the benefit of modulation doping, and it may be one important reason that allows the observation of the correlation peak in MDQW's, but not in doped, bulk semiconductors.

Summarizing this section, we have calculated the line shape of the absorption coefficient in the region of the absorption edge, using a many-body model to describe the eigenstates of the photoexcited electrons and holes and the Coulomb interaction between them in the presence of a background electron concentration. The result we obtain is that the absorption coefficient exhibits a singularity close to the Fermi edge, which broadens rapidly with increasing temperature or electron concentration. This behavior agrees with that observed experimentally, which allows us to identify the absorption edge peak in the modulation-doped quantum wells with the electron–hole correlation singularity (the Mahan exciton).

IV. Conclusions

We presented and discussed the temperature-dependent optical absorption and photoluminescence spectra of GaAs/AlGaAs and InGaAs/InAlAs n-doped MDQW's, and compared them to those of the undoped structures. In our analysis of the experimental data, we have concentrated on the effect of the free carriers on the subband structure, on one hand, and on the identification of the peak seen at the absorption edge, on the other. By self-consistently solving the Poisson and Schrödinger equations in the MDQW, we conclude that the electrostatic potential has negligible effects on the transition energies in these symmetrical structures in the case of moderate densities. We also find that these effects (such as they are) can be very well approximated by using the potential of a homogeneous distribution of the negative (electronic) charge in the quantum wells. Our second part of the discussion was devoted to the identification of the peak seen at the absorption edge in the spectra of the modulation-doped samples. We have shown that this peak may be identified with the many-body electron–hole correlation singularity (the Mahan exciton). Its appearance in the absorption spectra at an energy close to the Fermi edge is a consequence of the Coulomb interaction between the photoexcited hole and the sea of electrons. It is a manifestation of the screening: the movement of the electrons towards the hole to screen the potential of the hole of itself correlates them together, thus enhancing the absorption. This "correlation peak" becomes weaker and broadens with increasing temperature, reflecting the broadening of

the electrons' distribution function. The correlation also becomes weaker with increasing electron density as a result of the decreased electron–hole coupling due to increased phase-space occupation and exchange effects. The experimental spectra are in qualitative agreement with the theoretical predictions. The fact that this correlation singularity could not be seen in the absorption spectra of bulk-doped semiconductors, but can be observed in the spectra of the modulation-doped quantum wells, is, we believe, a result of the reduced scattering rate of the carriers in MDQW's. The Fermi edge correlation singularity is yet another manifestation of the very special properties of the free-electron gas in modulation-doped quantum well structures.

Acknowledgment

We wish to thank S. Schmitt-Rink, J. Shah, and C. Delalande, for many fruitful discussions, and J. E. Henry, D. J. Burrows, and A. E. DiGiovanni for expert technical assistance.

References

[1] For a relatively recent review, see A. C. Gossard and A. Pinczuk, "Modulation-doped semiconductors," in *Synthetic Modulated Structures*, L. L. Chang and B. C. Giessen, Ed. New York: Academic, 1985, pp. 215–255.

[2] A. Pinczuk, J. Shah, R. C. Miller, A. C. Gossard, and W. Wiegman, "Optical processes of 2D electron plasma," *Solid State Commun.*, vol. 50, pp. 735–739, 1984.

[3] R. C. Miller and D. A. Kleinman, "Excitons in GaAs quantum wells," *J. Luminescence*, vol. 30, pp. 520–540, 1985.

[4] A. E. Ruckenstein, S. Schmitt-Rink, and R. C. Miller, "Infrared and polarization anomalies in the optical spectra of modulation-doped semiconductor quantum-well structures," *Phys. Rev. Lett.*, vol. 56, pp. 504–507, 1986.

[5] M. H. Meynardier, J. Orgonasi, C. Delalande, J. A. Brum, G. Bastard, and M. Voos, "Spectroscopy of a high-mobility GaAs-$Ga_{1-x}Al_xAs$ one-side-modulation-doped quantum well," *Phys. Rev.*, vol. B34, pp. 2482–2485, 1986.

[6] C. Delalande, J. Orgonasi, M. H. Meynardier, J. A. Brum, and G. Bastard, "Band gap renormalization in a GaAs-$Ga_{1-x}Al_xAs$ modulation-doped quantum well," *Solid State Commun.*, vol. 59, pp. 613–617, 1986.

[7] C. Delalande, G. Bastard, J. Orgonasi, J. A. Brum, H. W. Liu, M. Voos, G. Weimann, and W. Schlapp, "Many-body effects in a modulation-doped semiconductor quantum well," *Phys. Rev. Lett.*, vol. 59, pp. 2690–2692, 1987; see also C. Delalande, "Optical properties of modulation doped quantum wells," *Physica Scripta*, and references therein, to be published.

[8] A. Petrou, G. Waytena, X. Liu, J. Ralston, and G. Wicks, "Photoluminescence study of a dilute two-dimensional electron gas in GaAs-$Al_xGa_{1-x}As$ quantum wells," *Phys. Rev.*, vol. B34, pp. 7436–7439, 1986.

[9] M. C. Smith, A. Petrou, C. H. Perry, J. M. Worlock, and R. L. Aggarwal, "Photoluminescence studies of Landau transitions in GaAs/AlGaAs multiple quantum wells," in *Proc. 17th Int. Conf. Phys. Semiconductors*, San Francisco, CA, 1984, J. D. Chadi and W. A. Harrison, Ed. New York: Springer-Verlag, 1985, pp. 547–550.

[10] F. Meseguer, J. C. Maan, and K. Ploog, "Luminescence of multiple modulation-doped GaAs-$Al_xGa_{1-x}As$ heterojunctions in high magnetic fields," *Phys. Rev.*, vol. B35, pp. 2505–2508, 1987.

[11] G. Livescu, D. A. B. Miller, and D. S. Chemla, "Electron-hole correlation singularity in optical spectra of modulation doped GaAs-AlGaAs quantum wells," *Superlattices Microstructures*, Mar. 1988.

[12] J. S. Lee, Y. Iwasa, and N. Miura, "Observation of the Fermi edge anomaly in the absorption and luminescence spectra of n-type modulation-doped GaAs-AlGaAs quantum wells," *Semiconductor Sci. Technol.*, vol. 2, pp. 675–678, 1987.

[13] D. Huang, R. Houdre, Y. C. Chang, and H. Morkoc, "Excitonic absorption in modulation-doped GaAs quantum wells," presented at the APS March Meet., New York, NY, 1987, paper PH2; also, *Bull. Amer. Phys. Soc.*, vol. 32, p. 850, 1987.

[14] M. S. Skolnick, J. M. Rorison, K. J. Nash, D. J. Mowbray, P. R. Tapster, S. J. Bass, and A. D. Pitt, "Observation of a many-body edge singularity in quantum well luminescence spectra," *Phys. Rev. Lett.*, vol. 58, pp. 2130–2133, 1987.

[15] M. S. Skolnick, K. J. Nash, P. R. Tapster, D. J. Mowbray, S. J. Bass, and A. D. Pitt, "Free carrier screening of the interaction between excitons and longitudinal optical phonons in $In_xGa_{1-x}As$-InP quantum wells," *Phys. Rev.*, vol. B35, pp. 5925–5928, 1987.

[16] M. S. Skolnick, K. H. Nash, M. K. Saker, S. J. Bass, P. A. Claxton, and J. S. Roberts, "Free carrier effects on luminescence linewidths in quantum wells," *Appl. Phys. Lett.*, vol. 50, pp. 1885–1887, 1987.

[17] D. S. Chemla, I. Bar-Joseph, C. Klingshirn, D. A. B. Miller, J. M. Kuo, and T. Y. Chang, "Optical reading of field-effect transistors by phase-space absorption quenching in a single InGaAs quantum well conducting channel," *Appl. Phys. Lett.*, vol. 50, pp. 585–587, 1987.

[18] I. Bar-Joseph, J. M. Kuo, C. Klingshirn, G. Livescu, T. Y. Chang, D. A. B. Miller, and D. S. Chemla, "Absorption spectroscopy of the continuous transition from low to high electron density in a single modulation-doped InGaAs quantum well," *Phys. Rev. Lett.*, vol. 59, pp. 1357–1360, 1987.

[19] W. H. Knox, D. S. Chemla, and G. Livescu, "High density femtosecond excitation of nonthermal carrier distributions in intrinsic and modulation doped GaAs quantum wells," in *Proc. 5th Int. Conf. Hot Carriers in Semiconductors*, Boston, MA, J. Shah and G. J. Jafrate, Ed., 1987. New York: Pergamon, 1988; also, *Solid State Electron.*, vol. 31, pp. 425–430, 1988.

[20] H. Lobentanzer, H. J. Polland, W. W. Ruhle, W. Stolz, and K. Ploog, "Cooling of an electron-hole plasma in a $Ga_{0.47}In_{0.53}As$ multiple quantum well structure," *Phys. Rev.*, vol. B36, pp. 1136–1139, 1987.

[21] D. S. Chemla and D. A. B. Miller, "Room-temperature excitonic nonlinear-optical effects in semiconductor quantum-well structures," *J. Opt. Soc. Amer. B*, pp. 1155–1173, 1985.

[22] See, for example, D. A. B. Miller, "Quantum wells for optical information processing," *Opt. Eng.*, vol. 26, pp. 368–372, 1987.

[23] E. Burstein, "Anomalous optical absorption limit in InSb," *Phys. Rev.*, vol. 93, pp. 632–633, 1954.

[24] S. Schmitt-Rink and C. Ell, "Excitons and electron-hole plasma in quasi-two-dimensional systems," *J. Luminescence*, vol. 30, pp. 585–596, 1985.

[25] R. Sooryakumar, D. S. Chemla, A. Pinczuk, A. C. Gossard, W. Wiegmann, and L. J. Sham, "Valence band mixing in GaAs-AlGaAs heterostructures," *Solid State Commun.*, vol. 54, pp. 859–862, 1985.

[26] R. Sooryakumar, A. Pinczuk, A. C. Gossard, D. S. Chemla, and L. J. Sham, "Tuning of the valence-band structure of GaAs quantum wells by uniaxial stress," *Phys. Rev. Lett.*, vol. 58, pp. 1150–1153, 1987.

[27] G. D. Mahan, "Excitons in degenerate semiconductors," *Phys. Rev.*, vol. 153, pp. 882–889, 1987; see also G. D. Mahan, "Excitons in metals: Infinite hole mass," *Phys. Rev.*, vol. 163, pp. 612–617, 1967.

[28] For an exhaustive theoretical treatment of the Mahan exciton in metals, see the series of papers by B. Roulet, J. Gavoret, and P. Nozieres, "Singularities in the X-ray absorption and emission of metals. I. First order parquet calculations," *Phys. Rev.*, vol. 178, pp. 1072–1083, 1969; P. Nozieres, J. Gavoret, and B. Roulet, "Singularities in the X-ray absorption and emission of metals. II Self-consistent treatment of divergencies," *Phys. Rev.*, vol. 178, pp. 1084–1096, 1969; and P. Nozieres and C. T. de Dominicis, "Singularities in the X-ray absorption and emission of metals. III. One-body theory exact solution," *Phys. Rev.*, vol. 178, pp. 1097–1107, 1969.

[29] S. Schmitt-Rink, C. Ell, and H. Haug, "Many-body effects in the absorption, gain and luminescence spectra of semiconductor quantum well structures," *Phys. Rev.*, vol. B33, pp. 1183–1189, 1986; for a discussion of the case of MDQW's, see A. E. Ruckenstein and S. Schmitt-Rink, "Many-body aspects of the optical spectra of bulk and low-dimensional doped semiconductors," *Phys. Rev.*, vol. B35, pp. 7551–7557, 1987.

[30] D. S. Chemla, D. A. B. Miller, P. W. Smith, A. C. Gossard, and W. Wiegmann, "Room temperature excitonic nonlinear absorption and refraction in GaAs/AlGaAs multiple quantum well structures," *IEEE J. Quantum Electron*, vol. QE-20, pp. 265–275, 1984.

[31] J. Weiner, D. S. Chemla, D. A. B. Miller, T. H. Wood, D. Sivco, and A. Y. Cho, "Room-temperature excitons in 1.6-μm band-gap GaInAs/AlInAs quantum wells," *Appl. Phys. Lett.*, vol. 46, pp. 619–621, 1985.

[32] W. H. Knox, C. Hirlimann, D. A. B. Miller, J. Shah, D. S. Chemla, and C. V. Shank, "Femtosecond excitation of nonthermal carrier populations in GaAs quantum wells," *Phys. Rev. Lett.*, vol. 56, pp. 1191-1193, 1986.

[33] D. A. B. Miller, D. S. Chemla, T. C. Damen, A. C. Gossard, W. Wiegman, T. H. Wood, and C. A. Burrus, "Electric field dependence of optical absorption near the band gap of quantum-well structures," *Phys. Rev.*, vol. B32, pp. 1043-1060, 1985; see also D. A. B. Miller, D. S. Chemla, and S. Schmitt-Rink, "Relation between electroabsorption in bulk semiconductors and in quantum wells: The quantum-confined Franz-Keldysh effect," *Phys. Rev.*, vol. B33, pp. 6976-6982, 1986.

[34] D. S. Chemla, I. Bar-Joseph, J. M. Kuo, T. Y. Chang, C. Klingshirn, G. Livescu, and D. A. B. Miller, "Modulation of absorption in field-effect quantum well structures," *IEEE J. Quantum Electron.*, this issue, pp. 1664-1676.

[35] D. J. Westland, A. M. Fox, A. C. Maciel, J. F. Ryan, M. D. Scott, J. I. Davies, and J. R. Riffat, "Optical studies of excitons in $Ga_{0.47}In_{0.53}As/InP$ multiple quantum wells," *Appl. Phys. Lett.*, vol. 50, pp. 839-841, 1987.

[36] W. Stolz, J. C. Maan, M. Altarelli, L. Tapfer, and K. Ploog, "Absorption spectroscopy on $Ga_{0.47}In_{0.53}As/Al_{0.48}In_{0.52}As$ multi-quantum-well structures. II. Subband structure," *Phys. Rev.*, vol. B36, pp. 4310-4315, 1987.

[37] The in plane masses of the heavy hole were calculated using the InGaAs valence-band Luttinger parameters from K. Alavi and R. L. Aggarwal, "Interband magnetoabsorption of $In_{0.53}Ga_{0.47}As$," *Phys. Rev.*, vol. B21, pp. 1311-1315, 1980.

[38] V. M. Asnin, V. I. Stepanov, R. Zimmermann, and M. Rosler, "Coulomb resonance at the Fermi level of the electron-hole liquid in germanium," *Solid State Commun.*, vol. 47, pp. 655-657, 1983.

Gabriela Livescu was born in Timisoara, Romania, in 1950. She received the B.Sc. degree from the University of Bucharest, Romania, in 1974 and the Ph.D. degree in physics from The Technion, Haifa, Israel, in 1984.

From 1984 to 1986 she was a Research Associate at the City College of New York, New York, before joining AT&T Bell Laboratories, Holmdel, NJ, in 1986, as a postdoctoral member of the Technical Staff in the Photonics Switching Research Department. She has recently become a member of the Technical Staff in the Department of Optoelectronics Devices, AT&T Bell Laboratories in Murray Hill, NJ. She has been engaged in experimental research on optical properties of ionic crystals and semiconductors. Her recent and current interests include linear and nonlinear spectroscopy of semiconductor quantum well structures.

David A. B. Miller, for a photograph and biography, see this issue, p. 1676.

D. S. Chemla (M'84), for a photograph and biography, see this issue, p. 1675.

M. Ramaswamy is a fourth year student in electrical engineering at the Massachusetts Institute of Technology, Cambridge. Her involvement in the experimental work leading up to the present paper occurred during the summer of 1987 when she was working at AT&T Bell Laboratories.

She is currently participating in M.I.T.'s Electrical Engineering Internship program with AT&T. She is working towards a joint Bachelors and Masters Degree in electrical engineering.

T. Y. Chang (S'62-M'70) was born in Taiwan, China, in 1937. He received the B.S. degree from the National Taiwan University, Taiwan, China, in 1959, the M.S. degree from Stanford University, Stanford, CA, in 1962, and the Ph.D. degree from the University of California, Berkeley, in 1966, all in electrical engineering.

From 1966 to 1967 he was an acting assistant professor at the University of California. He joined AT&T Bell Laboratories, Holmdel, NJ, in 1967 where he is now the supervisor of the MBE group in the microelectronics research department. His areas of research in the past included physics of magnetically confined plasmas, molecular gas lasers, far-infrared generation by optical pumping, and nonlinear optics. His current research interests include the growth of semiconductor heterostructures by molecular beam epitaxy and the physics and applications of these heterostructures.

Dr. Chang is a member of the American Vacuum Society and the Materials Research Society, and a Fellow of the Optical Society of America.

Nicholas Sauer was born in Albany, NY, in 1962. He received the B.A. degree in physics and chemistry from the State University of New York at Albany in 1984.

He joined Bell Laboratories in 1985. He is currently working on MBE growth of III-V structures.

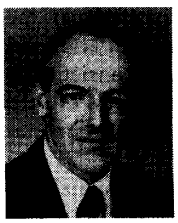

A. C. Gossard was born in Ottawa, IL. He received the B.A. degree in physics from Harvard University, Cambridge, MA, and the Ph.D. degree in physics from University of California, Berkeley.

Prior to 1987, he was a member of the Technical Staff at AT&T Bell Laboratories, Murray Hill, NJ, where he engaged in research on magnetic resonance properties of magnetic and metallic materials and on molecular beam epitaxy development of semiconductor quantum structures. Since 1987, he has been a Professor of Materials and Electrical and Computer Engineering at the University of California, Santa Barbara, where he is pursuing further research on the growth, properties and applications of quantum microstructures.

Dr. Gossard is a Fellow of the American Physical Society, a member of the National Academy of Engineering, and a recipient of the 1986 Oliver Buckley Condensed Matter Physics Award of the American Physical Society.

J. H. English, photograph and biography not available at the time of publication.